Desalination and Water Treatment
www.deswater.com

doi: 10.5004/dwt.2020.26430

207 (2020) 43–50
December

Enhancing performance of the membrane distillation process using air injection zigzag system for water desalination

Adnan Alhathal Alanezi[a,*], Yousef Alqahs Alanezi[a], Radhi Alazmi[a], Ali Altaee[b], Qusay F. Alsalhy[c], Adel O. Sharif[d]

[a]*Department of Chemical Engineering Technology, College of Technological Studies, The Public Authority for Applied Education and Training (PAAET), P.O. Box: 42325, Shuwaikh 70654, Kuwait, email: aa.alanezi@paaet.edu.kw (A. Alhathal Alanezi)*
[b]*School of Civil and Enviromental Engineering, University of Technology Sydney, Ultimo, NSW 2007, Australia*
[c]*Membrane Technology Research Unit, Chemical Engineering Department, University of Technology, Alsinaa Street 52, Baghdad, Iraq*
[d]*Centre for Osmosis Research and Applications (CORA), Chemical and Process Engineering Department, Faculty of Engineering and Physical Sciences, University of Surrey, Guildford GU2 7XH, UK*

Received 17 January 2020; Accepted 8 August 2020

ABSTRACT

A novel design of an air injection zigzag system was developed to enhance the tubular membrane distillation module's performance for desalination of water, unlike the basic design that works without an air injection system. Designed in a zigzag mode, the membrane distillation module is set to yield a high turbulence flow. Operating parameter effects, for example, the feed temperature (40°C, 50°C, 60°C, and 70°C), feed concentration (1, 3, and 5 g/L), and airflow rate (30–90 L/h), on process performance were investigated. The system proved its capability to enhance the heat and mass transfer coefficients. The basic and developed modules' performances were compared in terms of permeate flux (J_m) and thermal efficiency (η). The Reynolds number increased threefold, which consequently, increased the mass transfer coefficient by 25% and the heat transfer coefficient twofold compared to the basic module at airflow rate of 90 L/h. Moreover, the thermal efficiency and permeate flux were higher than the basic module's by roughly 1.4 and 1.5-fold, respectively, for a 5 g/L feed concentration.

Keywords: Tubular membrane; Membrane distillation; Air injection system, Desalination; Heat and mass transfer

1. Introduction

Water is one of the most fundamental resources needed to sustain life on Earth. Freshwater scarcity is one of the major global issues facing humanity today, especially in arid and semi-arid areas of the world, where clean drinking water can be obtained using a seawater desalination process [1–3]. The desalination process is where salt and other minerals are removed from seawater and brackish water in order to produce water suitable for consumption. Desalination can be achieved using several techniques, where globally about 80% of the World's desalination capacity is provided by multi-stage flash (MSF) and reverse osmosis (RO) [4–6]. However, these technologies intensively consume energy, mainly from fossil fuel, and are not linked to renewable energy sources. Membrane distillation (MD) stands amongst these new technologies with advantages over conventional desalination technologies, including operating at lower temperatures and pressures, more energy saving, and lower cost [1,7–9]. MD is a membrane-, thermal-based desalination process, wherein a hydrophobic micro-porous membrane splits water vapor from a liquid solution; the hydrophobic membrane allows the vapor to pass through it and prevents the liquids. Indeed, the driving force is the vapor

* Corresponding author.

pressure gradient resulting from a temperature variance between cold permeate and hot feed [7,10,11]. Many studies concentrated efforts to develop methods for improving the MD performance of permeate flux and thermal efficiency and decreasing the effect of polarization and membrane fouling [12]. Some researchers used spacers and baffles in membrane modules [13,14], whereas other researchers designed special rectangular cross-flow membrane modules [15,16]. The particular constructs of the modules of the membrane enhanced surface shear and flow turbulence; hence, the higher performance was achieved. The main objective of the current work is to enhance the performance of a tubular membrane module using a novel design of air injection membrane distillation process for water desalination. The effects of process variables on the developed performance were investigated. The basic module (without air) and the enhanced module (with air) were compared.

2. Experiment

2.1. Air injection tubular membrane module

An air injection tubular membrane module was designed and manufactured especially for enhancing the performance of the membrane distillation process. The air injection system was composed of four plastic tubes each 0.65 m long with 4 mm ID and small equidistant holes (1 mm) in each tube (as shown in Fig. 1), where the four tubes were arranged in a zigzag mode to increase the contact time for transporting vapor through membrane pores. The four plastic tubes were inserted and fitted inside four polymeric membranes of 0.65 m in length, 0.013 m in inner diameter, and 0.1061 m² total membrane effective area as shown in Fig. 1. Polytetrafluoroethylene (PTFE) hydrophobic membranes were supplied by Millipore Corporation, Mettler-Toledo, USA. The membrane properties of the supplied membrane are as follows; pore diameter of 0.2 µm, the thickness of 120 µm, the thermal conductivity of porosity of 75% as summarized in Table 1. The membrane has an

Table 1
Membrane properties

Membrane type	Polytetrafluoroethylene (PTFE)
Pore size (µm)	0.2
Thickness (µm)	120
Porosity (%)	75
Thermal conductivity (W/m K)	0.28

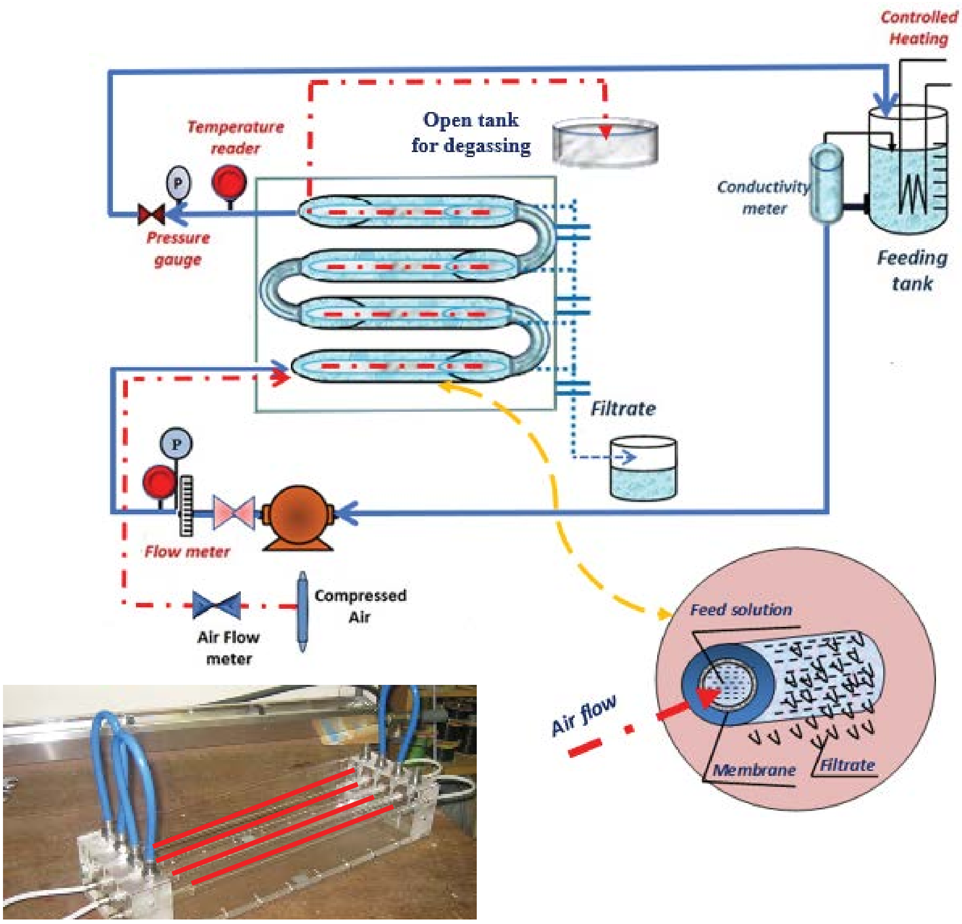

Fig. 1. Experimental setup air injection tubular membrane module.

operating pH range from 1.5 to 12, with water permeability of 0.475 and maximum pressure and temperature of 64 bar and 80°C. For cleaning the membrane, at a temperature of 40°C, 0.2 wt.% of nitric acid in distilled water can be used.

2.2. Experiment setup

The experiment setup for the air injection tubular module is presented schematically in Fig. 1. Pure and saltwater are transferred from the feeding tank, through the tubular module using a small diaphragm pump. Pressure gauges were positioned at the inlet and outlet of the membrane module in order to recycle the rejected stream to the feeding tank, where the saline feed conductivity was continuously recorded using thermal conductivity. Distilled water was added periodically to keep the saline solution concentration constant. The feed level was recorded with respect to time to estimate the evaporation rate, that is, the permeate flux. The feed flow rate was measured by a digital flow meter with a range of 60–240 L/h. Additionally, the feed temperatures are kept constant at (40°C, 50°C, 60°C, and 70°C) using a heater linked to a water bath. The inlet and outlet temperatures were measured using thermometer probes connected to the sides of the tubular membrane modules. Compressed air was introduced into the tubular membrane module to enhance the turbulent flow, where the outlet stream was sent to an open tank to remove the air from water and returning the water alone to the feed tank. The airflow rate was measured using a magnetic flow meter with range 30–90 L/h, while the air temperature (50°C) was measured and controlled by an electrical device (West 2050) connected to the membrane module.

2.3. Experiment procedures

To prepare the feed solution, measured crystals of sodium chloride (NaCl) were dissolved in deionized water to reach the required feed concentrations. The prepared solutions were utilized as standard saline solutions for the experiment. NaCl concentrations were calculated using a conductivity meter (Mettler Teledo). During experimentation, the permeate flux was measured every 10 min, where each run was active for 3 h. The average values of permeate flux for each run were computed at steady-state with the experimental error less than 5%. Permeate flux was calculated using the following equation:

$$J_m = \frac{\Delta V}{(A_m t)} \quad (1)$$

where J_m represents the permeate flux (kg/m^2 h), ΔV accumulated volume (L), A_m the membrane effective area (m^2), and t the running time (h).

3. Results and discussion

3.1. Accumulative produced water

The pure water experiments at a rate of 60 L/h were performed using compressed air at different flow rates 30–90 L/h and operated at different feed temperatures ranging from 40°C to 70°C. The accumulative water volume is defined as the amount of filtrate collected from the membrane module and the permeate flux was obtained by dividing the collected water volume to the membrane area and during a period of time. Fig. 2a shows a comparison between the accumulative water volume of the basic tubular module and the modified module using an air injection system at 60°C and 90 L/h of airflow rate. It is clear that the amount of accumulative produced water during the 3 h of operation was increased by the air injection system from 5% to 46% for the range of 30–90 L/h of airflow rate and 40°C–70°C of feed temperature, while maintaining feed flow rate constant at 60 L/h. This increase in the amount of collected water can be ascribed to the fact that the airflow rate will increase the turbulence over the membrane length. The turbulence increases the amount of heat supplied to the system using the hot feed water, which raises the water vapor diffusing through the membrane and improves both the mass and heat transfer processes; consequently, this increases the amount of accumulated water. In addition, with the enhancement of air bubbles, the mass transfer coefficient of MD is increased from 5% to 25% compared to the basic tubular membrane for the feed temperature and airflow rate ranging from 40°C to 70°C and 30 to 90 L/h, as shown in Fig. 2b. This may be related to the decrease in the mass transfer boundary layer resistance

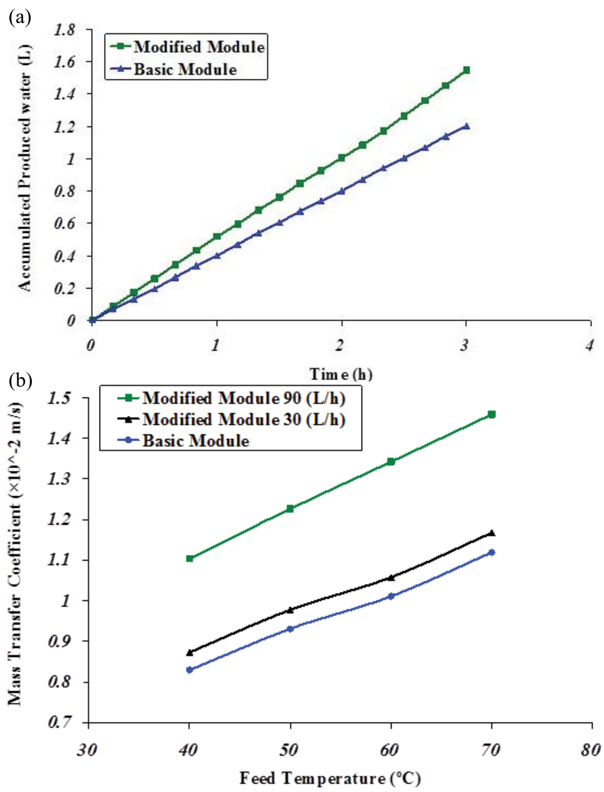

Fig. 2. (a) Comparison of accumulative produced water of basic and modified tubular modules vs. time at feed temperature of 60°C, 90 L/h airflow rate, and 60 L/h water feed flow rate. (b) Comparison of mass transfer coefficient of basic and modified tubular modules at different feed temperatures, airflow rates of 30 and 90 L/h, and 60 L/h water feed flow rate.

across the membrane module, which consequently increases the driving force, and increases the overall performance of the MD process. The experimental results of permeate flux (J_m) and thermal efficiency (η) are listed in Table 2.

3.2. Effects of process parameters

3.2.1. Effect of feed temperature

The feed temperature effect on the permeate flux in the air injection tubular membrane module was investigated, and compared to the basic tubular membrane module at 60 L/h water feed flow rate. The feed temperature effect on the performance of the basic and modified tubular MD modules at airflow rates 30 and 90 L/h are shown in Fig. 3a. The permeate flux of the modified tubular module with the enhancement of air injection system has increased from 13% to 18% for airflow rate ranging from 30 to 90 L/h and feed temperature of 40°C–70°C. Moreover, Fig. 3a shows that the permeate flux increased from 3% to 20% for airflow rate of 30 L/h, whereas it increased from 16% to 40% for the airflow rate of 90 L/h compared to the basic tubular module without air enhancement at feed temperature ranging from 40°C to 70°C. As expected, the higher feed temperatures increase the permeate flux exponentially as per the Antoine equation. The high feed temperature raises the diffusion of water vapor within the membrane pores, because of the increased mass transfer coefficient by up to 25%, as mentioned beforehand. In addition, the water temperature difference $\Delta T_{H_2O} = T_{in} - T_{out}$ flowing through the tubular module decreased due to the effect of air injection through the membrane. This result can be attributed to the fact that decreasing the temperature difference through the membrane length increases the mean temperature T_{mean} of bulk feed. This increases the vapor pressure gradient through the membrane, that is, increasing the driving force of the MD process, hence increasing the permeate flux. Moreover, increasing the mean temperature of the feed bulk will certainly increase the latent heat of water vaporization and increase the diffusion rate of water vapor passing within the membrane pores. Consequently, this increases the modified system's thermal efficiency compared to that of the basic tubular membrane. As shown in Fig. 3b, the thermal efficiency of the modified tubular module increased from 4% to 8% with the enhancement of the airflow rate from 30 to 90 L/h. In comparison to the basic module, the thermal efficiency increases from 20% to 40% for airflow rate of 30 L/h and from 30% to 50% for airflow of 90 L/h.

3.2.2. Effect of airflow flow rate

The experiments were performed for pure and saline solutions by changing the rate of airflow and feed temperature from 30 to 90 L/h and 40°C to 70°C, while maintaining the feed flow rate constant at 60 L/h. The airflow rate effect on permeate flux is presented in Table 3 and Fig. 4a. Referring to the previous facts, increasing the rate of airflow raises the permeate flux over the range of airflow rates. For instance, increasing the rate of airflow from 30 to 90 L/h resulted in a 3%–6% increase in the permeate flux. It is obvious that a double surge in airflow rates results in a small change in permeate fluxes. Therefore, an optimum airflow must be determined to acquire a high permeate flux. The increase of the permeate flux with airflow rate may be attributed to the increase in Reynolds number (Re), that is, turbulent regime. The turbulence increased as the mean velocity (m/s) of the air–liquid flow increased and the bulk liquid viscosity decreased as the mean temperature

Table 2
Permeate flux (J_m) and thermal efficiency (η %) at different operating parameters for modified tubular module at 60 L/h feed flowrate

	Feed temperature T_f (°C)								
	40		50		60		70		
F_{air} (L/h)	J_m (kg/m² h)					(η %)			C_f (mg/L)
30	1.26	35.2%	2.42	39.1%	4.00	45.3%	6.81	52.1%	
45	1.30	35.5%	2.58	40.9%	4.23	46.4%	7.23	53.8%	Pure water
60	1.37	36.5%	2.67	41.9%	4.41	47.7%	7.53	54.7%	
90	1.42	37.1%	2.78	42.5%	4.45	47.1%	8.00	56.3%	
30	0.67	21.6%	1.28	25.7%	2.20	31.6%	3.46	36.3%	
45	0.69	22.2%	1.36	26.5%	2.23	31.6%	3.66	37.2%	1,000
60	0.72	23.0%	1.41	27.2%	2.42	33.5%	3.83	38.3%	
90	0.75	23.7%	1.46	28.0%	2.52	34.3%	4.01	39.6%	
30	0.52	17.8%	1.15	23.0%	1.95	26.7%	3.35	33.4%	
45	0.54	18.1%	1.23	25.1%	2.08	28.0%	3.52	34.7%	3,000
60	0.57	18.8%	1.26	25.5%	2.15	28.9%	3.69	35.8%	
90	0.59	19.6%	1.31	25.8%	2.62	33.3%	3.89	36.8%	
30	0.45	15.9%	1.02	21.0%	1.84	25.9%	3.13	31.8%	
45	0.46	16.3%	1.09	22.2%	1.94	26.8%	3.34	33.2%	5,000
60	0.49	17.0%	1.12	22.4%	2.03	27.9%	3.46	34.1%	
90	0.51	17.4%	1.16	23.5%	2.13	28.7%	3.66	35.3%	

increased. Re increased by up to 25% as the airflow rate surged from 30 to 90 L/h. The enhancement in Re diminishes the mass transfer boundary layer resistance, in turn enhancing the mass transfer coefficient, thus leading to an increase in the permeate flux. In addition, the heat transfer coefficients increased with increasing Re, as shown in Table 3. This can be expected from the relationship of Re and Nusselt number to the heat transfer coefficients. Re increased by more than 76% and enhanced the heat transfer coefficient thus increasing it by more than 40%. In comparison with the basic tubular module, Re increased by more than threefold at 90 L/h airflow rate, which enhanced the heat transfer coefficient by more than two-fold with reference to the basic tubular module. The enhancement of the heat transfer coefficient affects the variation of inlet and outlet temperatures along the tubular membrane length, where the mean temperature increases proportionally with the heat transfer coefficient as it increases. This reduces the variance of temperature between the membrane surface and the feed bulk, resulting in an increase in the driving force, that is, the vapor pressure gradiant, and consequently, increases the permeate flux and thermal efficiency. Fig. 4b shows that the thermal efficiency of the modified module increased slightly by about 1% to 3% as the airflow rate increased from 30 to 90 L/h. Therefore, from the

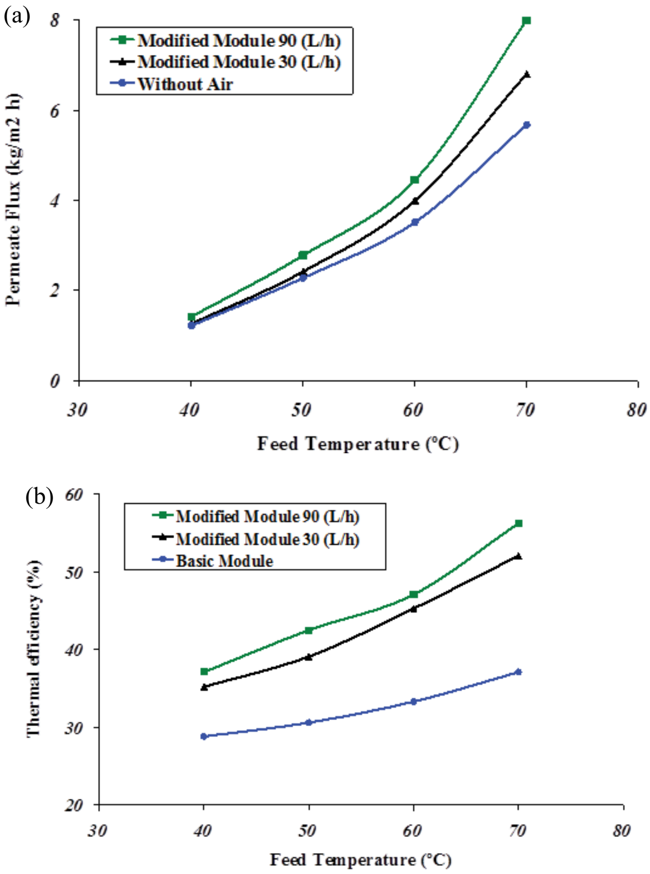

Fig. 3. Comparison of feed temperature effect on (a) permeate flux and (b) thermal efficiency of basic and modified tubular modules at 60 L/h water feed flow rate and airflow rates of 30 and 90 L/h.

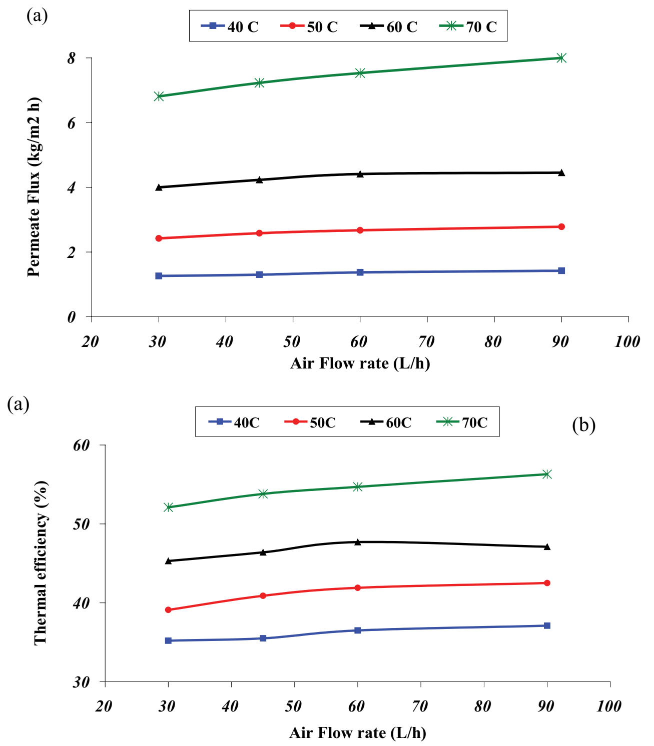

Fig. 4. Effect of airflow rate on (a) permeate flux and (b) thermal efficiency at different feed temperatures for water feed flow rate of 60 L/h.

Table 3
Comparison of Reynolds number effect on the heat transfer coefficients at feed boundary layer of basic and modified tubular modules at 60 L/h feed flowrate

	Without air		Air injection system (L/h)			
	60 (L/h)		30 (L/h)		90 (L/h)	
T_f (°C)	Re_f	h_f (W/m²K)	Re_f	h_f (W/m²K)	Re_f	h_f (W/m²K)
40	2,334	7,897	4,673	12,225	8,248	17,446
50	2,777	8,406	5,569	13,020	9,712	18,501
60	3,128	8,770	6,272	13,583	11,126	19,418
70	3,616	9,229	7,249	14,293	12,574	20,272

above results, it is obvious that the feed temperature effect on the permeate flux and thermal efficiency was found to be more significant compared to the effect of airflow rate.

3.2.3. Effect of feed concentration

The feed concentration of NaCl solution (1,000; 3,000; and 5,000 mg/L) effect on the thermal efficiency and permeate flux of the air injection system and the comparison with the basic tubular module are shown in Figs. 5a and b. During the experiments, the bulk feed temperature and airflow rate for the modified tubular module were maintained at each run at 40°C, 50°C, 60°C, and 70°C and 30, 45, 60, and 90 L/h. In this way, the feed concentration effect on the two processes' performance (basic and modified tubular modules) was investigated. Fig. 5a shows that at feed temperature of 70°C and airflow rate of 90 L/h, the permeate fluxes of both MD processes dropped as the feed concentration of NaCl surged. However, feed concentration effect on the permeate flux of the modified system was less compared to the basic tubular module. The permeate flux decreased by 9% (from 2.87 to 2.61 kg/m^{2}h) and 8% (from 4.01 to 3.66 kg/m^{2}h) for the basic and modified modules as the feed concentration increased from 1,000 to 5,000 mg/L. It must be mentioned that the modified system enhanced the permeate fluxes of the saline solution, but the declining percentage in the permeate flux was almost the same for both MD processes. The decline in the permeate flux as the feed concentration increased can be attributed to the increase in the boiling point of the salt solution. This decreases the latent heat of vaporization of water because of the additional layer developed on the membrane surface. In addition, according to Roult's law, increasing the salt concentration in the aqueous solution will lead to a decrease in the vapor pressure, the driving force across the membrane, and consequently, affects the permeate flux in the MD process. Fig. 5b illustrates that the feed concentration effect on the thermal efficiency of the two processes and the comparison between them at a feed temperature of 70°C and 90 L/h of airflow rate were as expected; the thermal efficiency decreased as the feed concentration increased from 1,000 to 5,000 mg/L. The thermal efficiency of the basic module decreased by about 6% (from 23.4% to 21.8%), while the thermal efficiency of the modified module decreased by 11% (from 39.6% to 35.3%), as the feed concentration increased from 1,000 to 5,000 mg/L. This reduction is due to the increase in temperature and concentration boundary layers, which consequently decreases the amount of heat flux required for vaporization Q_v. It must be mentioned that the amount of heat flux for vaporization for the basic and modified modules decreased by 9% and 8% at feed temperatures 70°C and 90°C (L/h) of airflow rate, as the feed concentration increased from 1,000 to 5,000 mg/L. Moreover, it is obvious that the thermal efficiency of the air injection system has increased by 70% for 1,000 mg/L and more than 60% for 5,000 mg/L compared to the basic tubular module. This can be attributed to the decrease in thermal boundary layer resistance, which consequently increases the amount of heat flux for evaporation Q_v of the modified tubular module, as seen in Table 4.

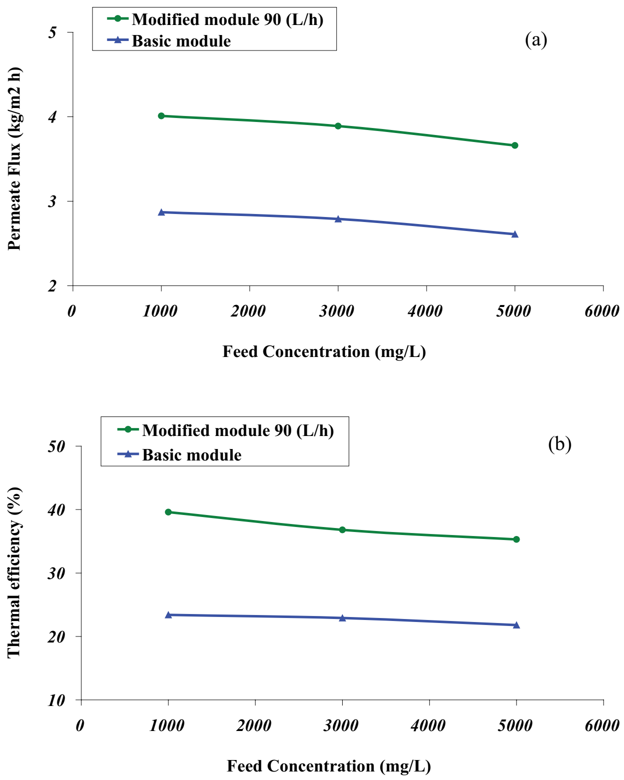

Fig. 5. Comparison of feed concentration effect on (a) permeate flux and (b) thermal efficiency of basic and modified tubular modules at 70°C, 60 L/h water feed flow rate, and 90 L/h airflow rate.

3.2.4. Effect of temperature polarization

Temperature polarization coefficients (TPC) at various feed temperatures, airflow rates, and feed concentrations are shown in Figs. 6a and b. Fig. 6a reveals the negative effect of feed temperature on TPC for the temperature range from 40°C to 70°C, airflow rates of 30 and 90 (L/h), and 5,000 mg/L, where the values of TPC range from 0.986 to 0.984. Clearly, TPC decreased as the feed temperature increased owing to the exponential rise of the vapor pressure with temperature (according to the Antoine equation). Moreover, higher temperature results in higher energy consumption due to the evaporation of liquid phases at the feed membrane surface. However, Fig. 6b shows enhancement in TPC for the air injection flow rate range from 30 to 90 L/h at 5,000 mg/L feed concentration and feed temperatures of 40°C and 70°C. The TPC increased at higher airflow rates due to the increase in Re and heat transfer coefficient as mentioned above which consequently decreases the thermal boundary layers at the feed side, where the increase in airflow rate from 30 to 90 L/h at 40°C and 5,000 mg/L enhanced the TPC from 0.980 to 0.986. Fig. 7 presents the comparison between the modified tubular and basic tubular modules in terms of TPC at different feed temperatures ranging from 40°C to 70°C, 150 L/h airflow rate for the modified module, and 5,000 mg/L feed concentration. The TPC improved for the air injection system at 90 L/h, where the TPC of the modified system increased compared

Table 4
Comparison of evaporation heat flux of basic and modified tubular modules for pure and saline water at different feed temperatures at 60 L/h feed flowrate

Q_v (W/m²K)						
C_f	Pure water		1,000 mg/L		5,000 mg/L	
T_f (°C)	Without air	Airflow of 90 L/h	Without air	Airflow of 90 L/h	Without air	Airflow of 90 L/h
40	823.0	958.0	432.0	506.0	290.0	344.0
50	1,531	1,867	806.0	981.0	645.0	779.0
60	2,355	2,976	1,292	1,684	1,084	1,423
70	3,782	5,328	1,913	2,667	1,739	2,434

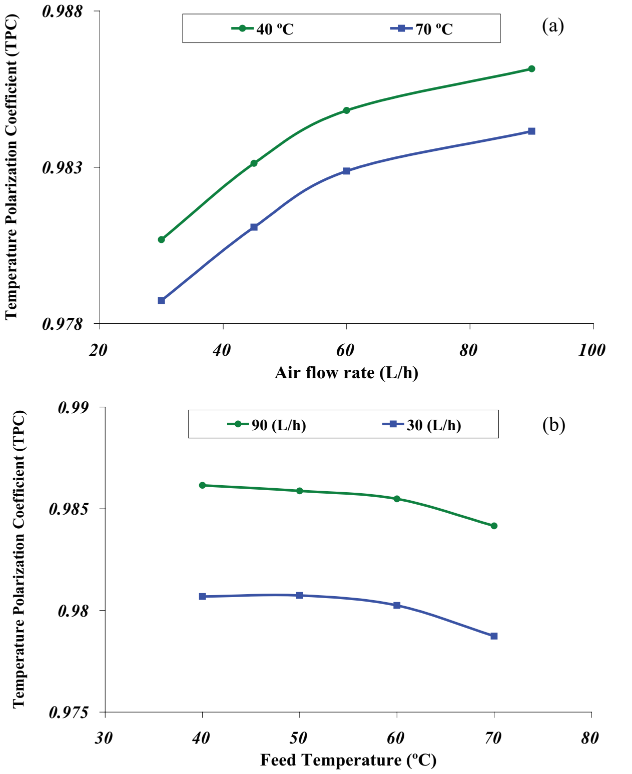

Fig. 6. Temperature polarization coefficients (TPC) vs. (a) airflow rate and (b) feed temperatures at 60 L/h water feed flow rate and 5,000 mg/L feed concentration.

to the basic module from 0.962 to 0.986 at 40°C and from 0.956 to 0.984 at 70°C.

4. Conclusion

On the basis of tubular membrane module performance, some modifications to the basic tubular membrane were undertaken. The modified module uses an air injection system for improving the flow conditions and for strengthening the operation of the heat and mass transfer at the feed side. The experiment results showed that the amount of cumulatively produced water increased from 5% to 46%. In addition, with the enhancement of air bubbles, the mass transfer coefficient of MD increased from 5% to 25% compared to the basic tubular membrane at different feed temperatures (40°C–70°C). It was concluded that the performance of the process in terms of permeate flux increased from 13% to 18% and 20% to 50% in terms of thermal energy efficiency. Furthermore, it can be concluded that there is no need to use high airflow rates because the results showed only a slight improvement in permeate flux (3%–6%) and 4%–8% in thermal efficiency for airflow rate increases from 30 to 90 L/h. Therefore, optimum airflow must be determined to achieve high MD performance. For the feed concentration effect, it was concluded that the modified system enhanced the permeate fluxes of the saline solution, but the decline in percentage in permeate flux was almost the same for both modules. The TPC improved when using the air injection system, and its values were 0.984–0.986. Based on the experimental results we can conclude that the air injection MD process can open an interesting prospective for practical applications in MD field because the membrane system is modular and can therefore be scaled up easily. Additionally, the membrane elements are of tubular configuration which also makes scaling up with a reduced footprint easier. Moreover, the availability of air can be safely used to reduce the membrane fouling and enhance the performance steadily.

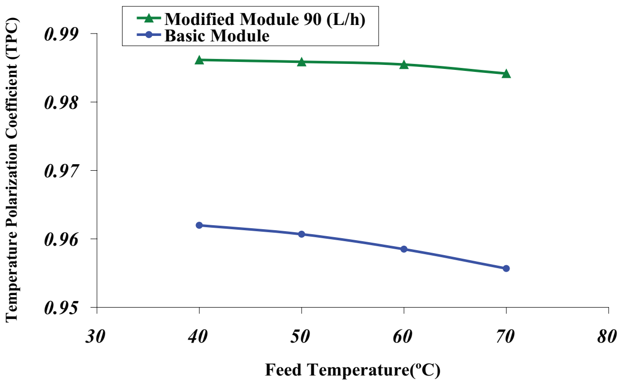

Fig. 7. Comparison of temperature polarization coefficient (TPC) of basic and modified module at 90 L/h airflow rate for 5,000 mg/L feed concentration and 60 L/h water feed flow rate.

Acknowledgment

The authors wish to express their sincere thanks to the Public Authority of Applied Education (PAAET) in Kuwait for funding this research during sabbatical leave.

References

[1] A. Alhathal Alanezi, A.O. Sharif, M. Sanduk, A. Khan, Potential of membrane distillation-a comprehensive review, Int. J. Water, 7 (2013) 317–346.

[2] A. Alhathal Alanezi, Y. Elhenawy, M.R. Safaei, M. Goodarzi, The effect of inclination angle and Reynolds number on the performance of direct contact membrane distillation (DCMD) process, Energies, 13 (2020) 1–16, doi: 10.3390/en13112824.

[3] Y. Elhenawy, N.A.S. Elminshawy, M. Bassyouni, A. Alhathal Alanezi, E. Drioli, Experimental and theoretical investigation of a new air gap membrane distillation module with a corrugated feed channel, J. Membr. Sci., 594 (2020) 1–13, doi: 10.1016/j.memsci.2019.117461.

[4] A. Alhathal Alanezi, A. Altaee, A. Sharif, The effect of energy recovery device and feed flow rate on the energy efficiency of reverse osmosis process, Chem. Eng. Res. Des., 158 (2020) 12–23.

[5] J. Kavitha, M. Rajalakshmi, A.R. Phani, M. Padaki, Pretreatment processes for seawater reverse osmosis desalination systems – a review, J. Water Process Eng., 32 (2019), doi: 10.1016/j.jwpe.2019.100926.

[6] A. Altaee, J. Zhou, A. Alhathal Alanezi, G. Zhao, Chapter 4: Design and Optimization for a Closed-Loop Pressure Retarded Osmosis Process, J.E. Peter, Ed., Energy Efficiency: Performance, Improvement Strategies, and Future Directions, Nova Science, USA, 2017, pp. 65–90.

[7] A. Alhathal Alanezi, A.O. Sharif, M.I. Sanduk, A.R. Khan, Experimental investigation of heat and mass transfer in tubular membrane distillation module for desalination, ISRN Chem. Eng., 2012 (2012) 1–8.

[8] A. Alhathal Alanezi, A.O. Sharif, Membrane distillation: an attractive alternative, Arab Water World, 36 (2012) 16–19.

[9] N.M. Mokhtar, W.J. Lau, A.F. Ismail, The potential of membrane distillation in recovering water from hot dyeing solution, J. Water Process Eng., 2 (2014) 71–78.

[10] A. Alhathal Alanezi, H. Abdallah, E. El-Zanati, A. Ahmad, A.O. Sharif, Performance investigation of O-ring vacuum membrane distillation module for water desalination, J. Chem., 2016 (2016) 1–11 pages.

[11] M.J. Jamed, A.A. Alhathal Alanezi, Q.F. Alsalhy, Effects of embedding functionalized multi-walled carbon nanotubes and alumina on the direct contact poly(vinylidene fluoride-co-hexafluoropropylene) membrane distillation performance, Chem. Eng. Commun., 206 (2018) 1035–1057.

[12] X. Yang, R. Wang, A.G. Fane, Novel designs for improving the performance of hollow fiber membrane distillation modules, J. Membr. Sci., 384 (2011) 52–62.

[13] J. Phattaranawik, R. Jiraratananon, A.G. Fane, C. Halim, Mass flux enhancement using spacer filled channels in direct contact membrane distillation, J. Membr. Sci., 187 (2001) 193–201.

[14] L. Martínez, J.M. Rodríguez-Maroto, Characterization of membrane distillation modules and analysis of mass flux enhancement by channel spacers, J. Membr. Sci., 274 (2006) 123–137.

[15] M.M. Teoh, S. Bonyadi, T.-S. Chung, Investigation of different hollow fiber module designs for flux enhancement in the membrane distillation process, J. Membr. Sci., 311 (2008) 371–379.

[16] M. Peydayesh, P. Kazemi, A. Bandegi, T. Mohammadi, O. Bakhtiari, Treatment of bentazon herbicide solutions by vacuum membrane distillation, J. Water Process Eng., 8 (2015) e17–e22.